ARTICLE IN PRESS

Available online at www.sciencedirect.com

SCIENCE DIRECT®

Sensors and Actuators A xxx (2004) xxx–xxx

SENSORS AND ACTUATORS A PHYSICAL

www.elsevier.com/locate/sna

Electrostatic actuated micro gripper using an amplification mechanism

Olivier Millet [a,*], Paul Bernardoni [b,c], Stéphane Régnier [b,c], Philippe Bidaud [b,c], Elli Tsitsiris [c], Dominique Collard [d], Lionel Buchaillot [a]

[a] *Institut d'Electronique, de Micro-électronique et de Nanotechnologie IEMN, Dept. ISEN, IEMN, UMR CNRS 8520, Avenue Poincaré, Cité scientifique, 59650 Villeneuve d'Ascq, France*

[b] *Laboratoire de Robotique de Paris LRP, 18, rue du panorama, 92265 Foxteney-aux-noses, France*

[c] *Commissariat à l'Energie Atomique, 18, rue du panorama, 92265 Foxteney-aux-noses, France*

[d] *Center for International Research on MicroMechatronics CIRMM, 18, rue du panorama, 92265 Foxteney-aux-noses, France*

Received 1 July 2003; received in revised form 28 October 2003; accepted 1 November 2003

Abstract

This paper presents a microgripper using an amplification mechanism coupled to an electrostatic linear motor. The gripper design, particularly the principle of the amplification mechanism based on the combination of ground-links and moving pin-joints, is explained. The linear motor is composed of scratch drive actuator inducing the use of electrostatic forces to obtain quasi-static motion for high accuracy in micropositioning. To corroborate the design, the gripper mechanism has been modeled by finite elements method with different mesh elements via the simulator CASTEM 2000$^{\text{TM}}$. Then, the amplification ratio of displacement, the critical buckling load and the force applied to the grasped object are determined. Moreover, the fabrication process requiring four levels of polysilicon are presented and notices based on visual observations of the realized actuator are given. Based on video observations, kinematics characterization of different topologies of the microgripper is performed and a discussion concerning the comparison with the simulation results and the influence of the geometric shapes of jaws/arms on the kinematics parameters is done. Finally, reliability aspects are stated consisting in the determination of the brittleness areas.

Keywords: Microgripper; Amplification mechanism; Quasi-static motion; Micropositioning; Scratch drive actuator; Electrostatic actuation

1. Introduction

A miniature gripper may be of interest in order to insure safe transport of small objects as electronic devices, to have a new tool to grasp cells for bio-application and to get end-effectors for endoscope manipulations. The specifications to realize such a gripper is to obtain quasi-static motion to have high accuracy in micropositioning, a large-stroke micro-actuator to grasp the maximum types of object, and the use of electrostatic forces in order to avoid high power consumption. In the last decade, microtechnologies have already provided demonstrators of electrostatic microgrippers but their low aspect ratio did not allow the safe transportation of micro objects [1]. Moreover, up to now, the quasi-static motion had not been performed via the use of electrostatic forces which were more useful for the generation of vibrating motion [2]. Shape memory alloys (SMA) allows high accuracy in micropositioning and have great advantages such as large deformation, strong recovery force and a high work density; the literature reports some examples of microfabricated gripper or clipping structure [3–5]. Alternatively, piezoelectric actuators have also been used to perform accurate micropositioning [6]. Finally, pneumatic microgrippers present several advantages like high generated forces and excellent dynamic behaviour [7,8].

In the present work, a linear motor consisting in a train composed of 16 scratch drive actuators (SDAs) has been used to drive an amplification mechanism, in order to decrease the ratio of the arms displacement to the area filled by the whole system compared to the existing microgrippers [2–8]. SDAs are well-known transducers converting electrostatic forces into friction mechanical forces, such an operating principle allows achieving high accuracy positioning with a controllable velocity [9]. This double accuracy is also used in the presented system to perfectly monitor the grip action of any object without damaging it: compared to

* Corresponding author. Tel.: +33-320-19-7838; fax: +33-320-19-7884.
E-mail address: lionel.buchaillot@isen.fr (L. Buchaillot).

0924-4247/$ – see front matter © 2003 Elsevier B.V. All rights reserved.
doi:10.1016/j.sna.2003.11.004

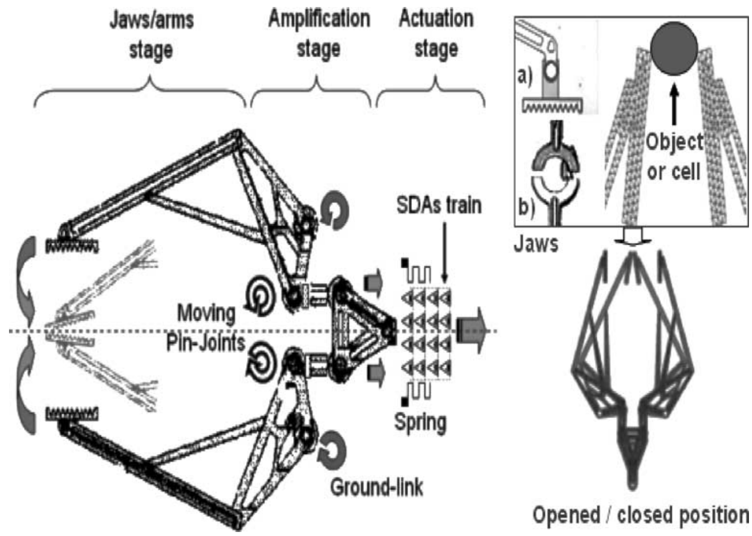

Fig. 1. Microgripper mechanism with the three different parts: actuation stage, amplification stage with different jaws design (a–b).

SMA or pneumatic actuators [3–5,7,8], the generated forces are not high in order not to damage biological materials. At last, the use of SDAs allows the use of electrostatic forces to perform quasi-static motion.

In this paper, first, the three stages of the designed micro-gripper (actuation, amplification, jaws) are described and the principle of the amplification mechanism is explained. Then the fabrication process consisting in surface micromachining with polysilicon as structural layer is shown. In order to optimize the design, analyses have been performed by using finite element method (FEM) to model the system. CASTEM 2000$^{\mathrm{TM}}$ has allowed a precise evaluation of the functioning system and has avoided design mistakes involving no phenomenon such as buckling and ruptures; different approaches (mesh elements in FEM analysis) have been used to quantify the risks of these critical phenomena. Next, kinematics characterization of different types of grippers (shapes of the arms and jaws) has been established: experimental results agree well with simulations.

2. Design

As explained previously, the whole system is the combination of three stages: actuation, amplification mechanism and jaws/arms stage. The actuation stage consists in a train of 16 SDAs (Fig. 1); SDAs shape is a triangle with 70 μm sides. Buried electrodes are placed underneath the train in order to use electrostatic forces to actuate the linear motor. Two springs attach the motor to the contact pads (Fig. 1). The goal of this stage is that under actuation, the resulting pulling forces induce the linear displacement of the coupled amplification mechanism. The amplification stage is the

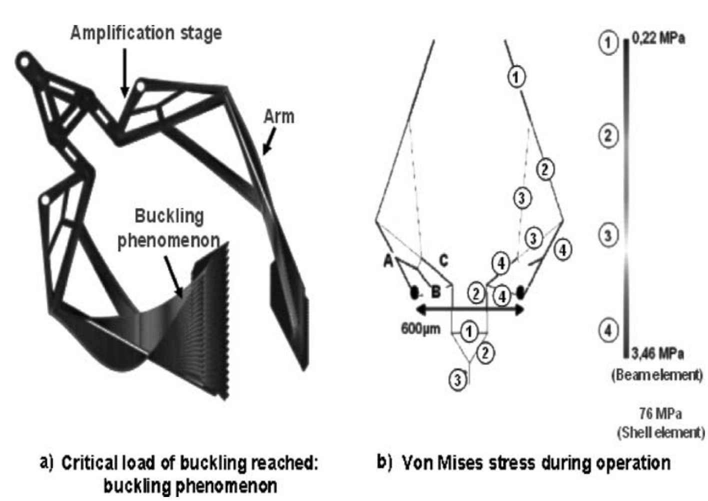

Fig. 2. Simulation by FEM of the buckling phenomenon (a) and analysis of Von Mises stress in the structure during operation (b).

combination of two ground-links and five moving pin-joints (Fig. 1). The two ground-links are the hubs of the rotating arms and are useful to ground the overall mechanical structure to the substrate. Three moving pin-joints are use to limit the stress due to the induced torque when the SDAs train pulls. The two others allow the rotation of the arms around the ground-links. The amplification ratio is defined as the ratio of one gripper arm displacement to the SDAs train displacement. The first goal of this stage is to increase the total rigidity of the structure in order to avoid buckling phenomenon, and secondly to increase the amplification ratio to decrease the area filled by the gripper. The last stage is composed of two arms with jaws at each extremity. The shape of jaws and arms depends on the nature and the size of the grasped object. Fig. 1a and b, respectively show jaws for the secure transport of a polymer object and jaws for grasping optical fiber.

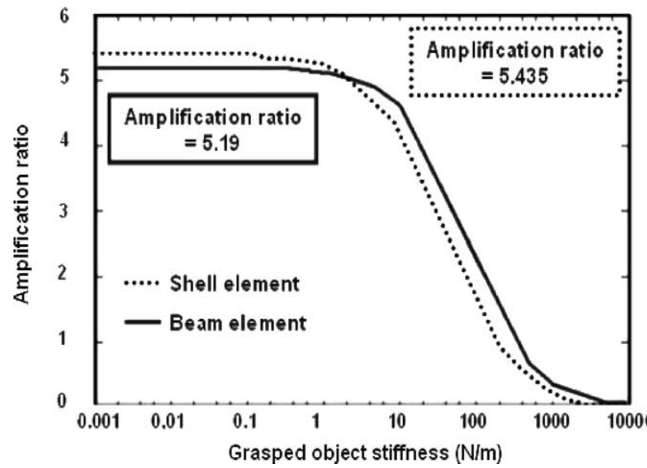

Fig. 3. Evolution of the amplification ratio vs. the grasped object stiffness according to the used mesh element (beam, shell).

3. Simulations

The simulations of the gripper have been performed with CASTEM 2000™ which is a simulator using the FEM. Two approaches have been used to simulate the structure, consisting in the choice of shell or beam elements for the mesh of the structure. Next, the simulations results obtained in the both cases are presented. For simulations, the force developed by one SDA is assumed to be equal to 50 μN [5]. The first step has been to determine the critical parameters: the critical load of buckling (Fig. 2a) and the induced stress during operation (Fig. 2b). The critical load of buckling is equal to 3040 μN in the case of beam elements and 1360 μN with shell elements, leading to a minimum security factor of 1.7. So, buckling is avoided during actuation. Concerning the induced stress, the Von Mises stress is presented in Fig. 2b and highest stress level is found in arms crossing area *S* (Fig. 2b) (other parts having low induced stress) with 3.5 MPa (beam elements) and 129 MPa (shell elements) which is far below the yield stress of polysilicon (1.2–1.5 GPa); indeed, no ruptures can appear during the functioning of the gripper. Secondly, the evolution of the amplification ratio versus the grasped object stiffness has been analyzed (Fig. 3). Whatever the mesh element, two steps can be observed: first the amplification ratio is constant and next it decreases. For the aimed applications, i.e. cells or polymer objects grasping, the amplification ratio is constant and equal to 5.19 (beam element) or 5.435 (shell element). Finally, sensitivity of the microgripper depends on the arm stroke and Fig. 4 shows the displacement of one arm with respect to the force generated by SDAs for different object stiffness; stiffness of some materials are shown in order to get stiffness reference points. These simulation results allow pointing out that, in the case of small stiffness of the object to grasp, only four SDAs are required to actuate the gripper; but, in order to be sure to overcome stiction and friction phenomena, 16 SDAs compose the pulling train.

4. Fabrication

The polysilicon microgripper, fabricated with the conventional surface micromachining technology, requires eight mask levels. Four levels of polysilicon are needed: three as structural layers to fabricate the moving pin-joints and one for the buried electrodes. The smallest dimension of the mask pattern is equal to 3 μm. A 5–20 $\Omega\,cm^{-1}$ P type (1 0 0) silicon wafer was used as the substrate. For the sake of clarity, Fig. 5 depicts the process fabrication, for one polysilicon structural layer whereas the structures fabrication needs three structural layers. A 0.35 μm oxidation is performed (Fig. 5a). LPCVD *n*-doped polysilicon is then deposited (0.35 μm). After electrode patterning (Fig. 5b), the polysilicon is oxidized (Fig. 5c) and covered with a low stress LPCVD Si_xN_y layer (0.35 μm) (Fig. 5d). A 2 μm low temperature oxide (LTO) was deposited (Fig. 5e) followed by the etching of SDA bushing (1.5 μm) and contacts (Fig. 5f). A 2 μm LPCVD polysilicon was deposited followed by the deposition of phosphorus silicon glass (PSG 1 μm). After diffusion of the dopants, PSG was removed using HydroFluoridric (HF) (Fig. 5g). SDAs are made of the first structural layer, so the polysilicon was thinned from 2 to 0.5 μm by SF_6 plasma in order to lower the SDAs stiffness and the resulting driving voltage. The structural pattern was defined by SF_6, CF_4 and O_2 reactive ion etching (RIE) (Fig. 5h). Then, a 2 μm LTO was deposited followed by the etching of contacts. Two micrometers of LPCVD polysilicon was deposited and the structural pattern was delineated by SF_6, CF_4, O_2 etching. Finally a 2 μm LTO is deposited. The etching of contact holes was performed. As before, a 2 μm LPCVD polysilicon was deposited and patterned by RIE. Next the structure was annealed at 1000 °C for 3 h to relax residual stress. Finally, the structure has been released using HF (Figs. 5i and 6).

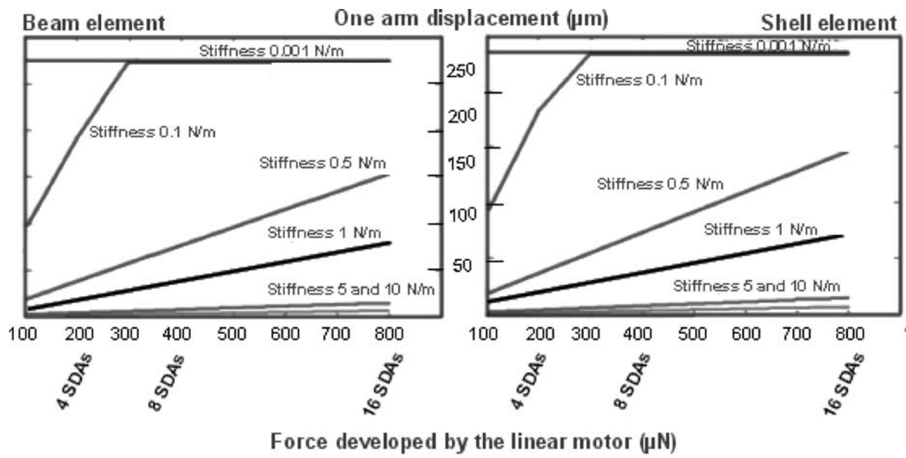

(a)

Material of the grasped object	Stiffness N/m	Material of the grasped object	Stiffness N/m
steel	3,14E+05	skin 2	47
lead	26650	rubber	15,7
nylon	4390	polymere gel	1,57E-02
polyethylene	314	chromosome	4,70E-04
skin 1	172	endothelilale cell	2,04E-04
lysozyme molecule 1	2,04	lysozyme molecule2	0,705

(b)

Fig. 4. Displacement of one arm gripper arm vs. the force generated by the SDAs train as a function to the grasped object stiffness and according to the mesh element (beam, shell) (a) and reference points of stiffness values (b).

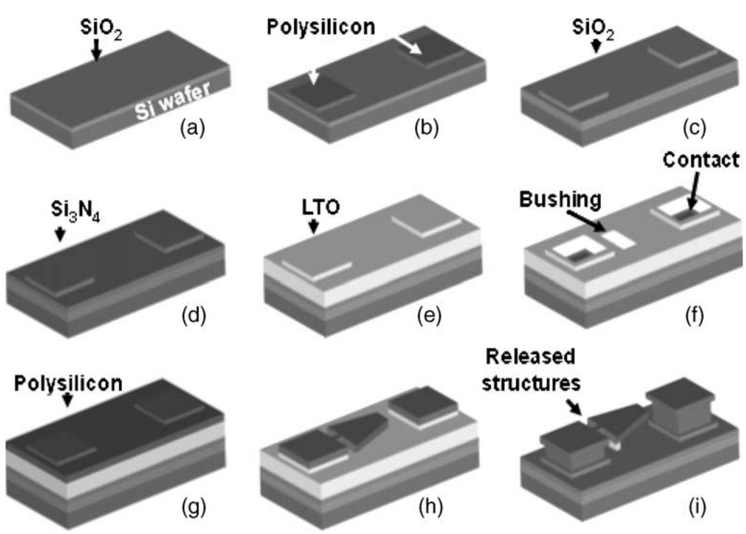

Fig. 5. Fabrication process consisting in surface micromachining with polysilicon as structural layer.

5. Observations of the gripper

Scanning electron microscope pictures of the gripper are displayed on Fig. 6. The microgripper dimensions are $1200 \times 800\ \mu m^2$. The three stages can be observed (Fig. 6a) and several observations can be done. First, a detail of a ground-link shows that no planarization step has been performed during the fabrication (Fig. 6b). Secondly, the flexible springs which biased the SDAs are the only parts of the system which would force the gripper to be opened up again after actuation, but the restoring force of the springs is small compared to the friction/stiction force [10,11]. So, in this design version, the microgripper can only perform one operation. The advantage of this topology is that the grasp of an object is perfectly controlled: the actuation of the gripper can be stopped at any time, letting then the gripper closed up in the

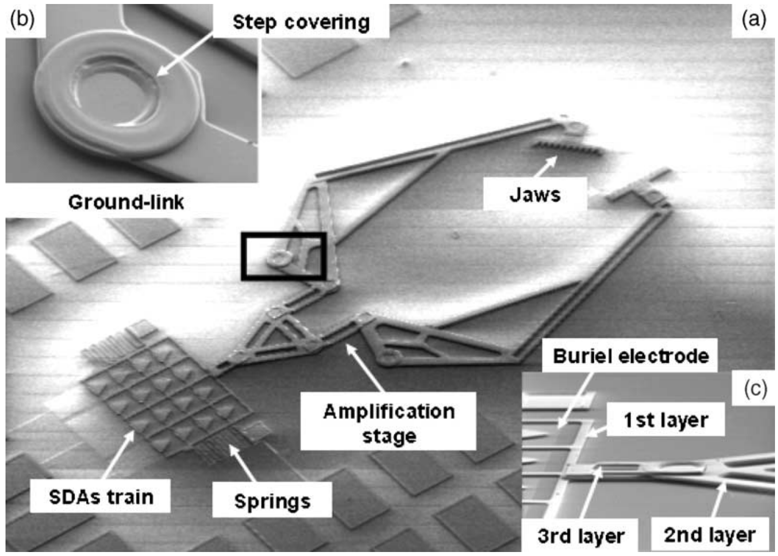

Fig. 6. Electrostatic microgripper, combination of a linear motor, an amplification mechanism and a grasping stage (a), with the detail of a ground-link (b) and the visual observation of the four polysilicon layers (c) required to fabricate the mechanical structure.

desired position. This is useful to achieve a secure transport or to immobilize a cell without damaging it. Afterwards, Fig. 6c allows the observation of the four polysilicon layers and a detail of a moving-pin joint; the first thinned polysilicon layer can be visually compared to the thickness of the addition of the three structural layers at the link between the motor and the amplification mechanism. Finally, the fabrication of a reservoir underneath the gripper has been done (Fig. 7) for two reasons; the first one is to perform biological experiments such as cell clamping in aqueous solution and the second one is to reduce the surface interaction between the grasping arms and the substrate in order to decrease the friction phenomenon. The etching of the reservoir has been post-processed (Fig. 7a). A window was defined via a BE7-1 wet etching step in order to access the silicon nitride layer (Fig. 7b). The silicon nitride was etched by CHF_3 and CF_4 (Fig. 7c) in order to etch the thermal oxide during the releasing (Fig. 7d). The reservoir is 0.9 μm in depth.

6. Experiment and discussion

Two different types of gripper have been actuated: the first one having for goal to transport polymer objects (simulated structure) and the second designed for grasping optical fiber (not simulated by CASTEM 2000™). In both cases, pulsed

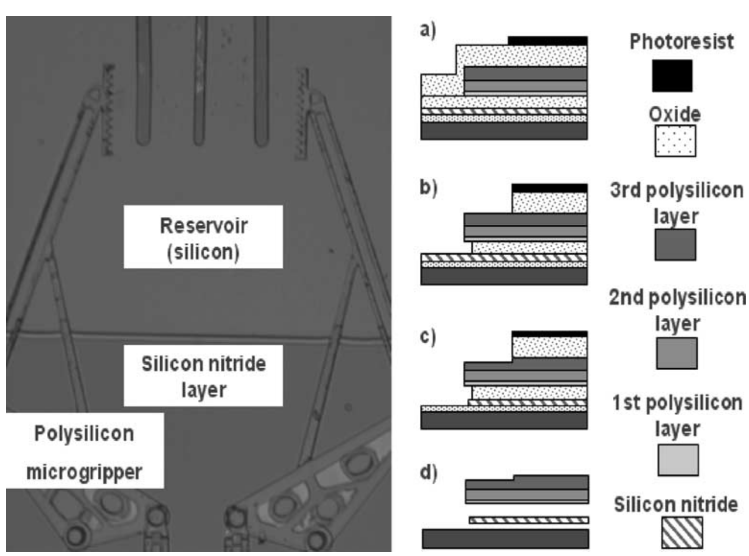

Fig. 7. Observation and post-process etching of a reservoir underneath the mechanical structure for biological applications and for decreasing surface interaction between the gripper arms and the substrate.

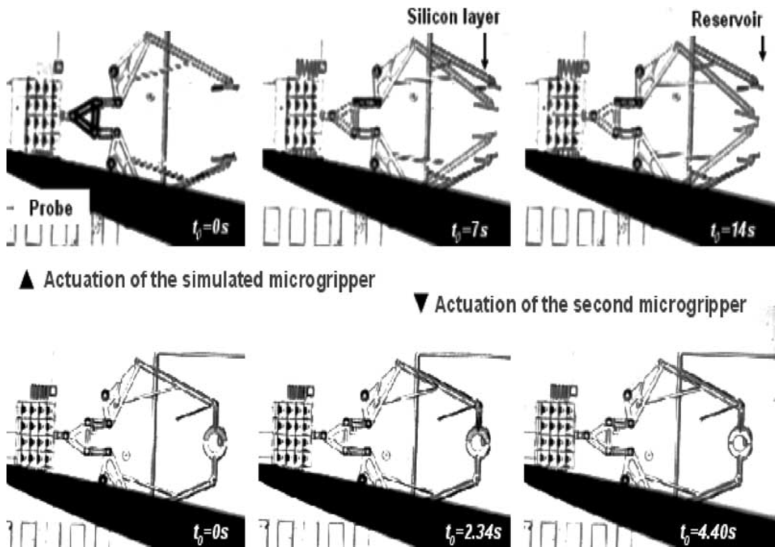

Fig. 8. Video observations of two different microgrippers during operation. (a) Simulated gripper used for the safe transport of polymer objects, (b) gripper for grasping optical fiber.

voltages of ±75 V for SDA actuation allow to overcome the initial surface adhesion forces, such as surface stiction and electronic coupling, and to pull the amplification stage. The actuation frequency of SDAs was set to 45 Hz and tests have been performed in the air.

Fig. 8 shows some observations during functioning of the two microgrippers. It can be seen the rest of the nitride layer which were masked by polysilicon gripper during the reservoir etching (Fig. 7c and d). After actuation, without applied voltage, the grippers remain in closed up position as expected.

Kinematics characterization has been performed through video observation and it confirms results given by the simulation in terms of displacement and amplification ratio in the case of the simulated structure: the amplification ratio has been determined equal to 5.90 (5.19 or 5.435 in theory). The difference can be explained by the fact that the spaces between the hubs and the moving parts are not taken into account during the simulation step and that the shape of the jaws is different. Finally, shell elements for the mesh in the FEM analysis seem more suitable for simulation step. From the non-simulated gripper, the amplification ratio is equal to 2.5.

Assuming that $t_0 = 0$ s is the beginning of the gripper motion, the displacement of one arm versus the time is reported in Fig. 9 for the two grippers. Experimental results show that the grippers is closed up after 14 s and that the speed is constant (19.64 μm/s) in the case of a displacement of 275 μm for one gripper arm. In the case of the non-simulated microgripper, the speed is constant an equal to 4.625 μm/s. It appears that the larger the stroke is, the more the speed of grasping is increased.

The experiments show that the kinematics parameters and the amplification ratio of the gripper depend on the shape of the jaws/arms stage; so, for each new design, simulations

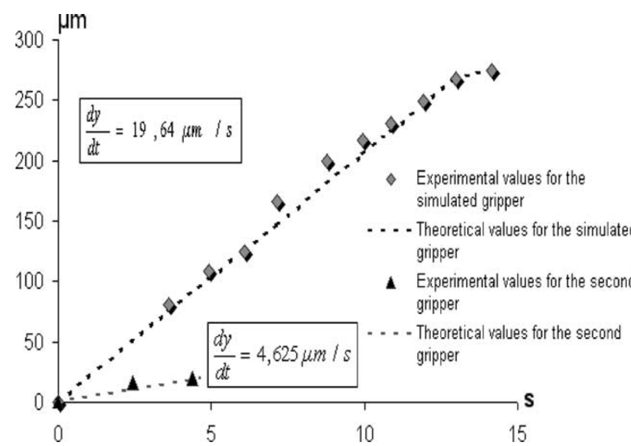

Fig. 9. Experimental measurements of one arm displacement vs. the time in the case of each actuated microgripper and determination of the grasping speed.

have to be performed to determine the amplification ratio. Finally, actuation parameters are exactly the same.

7. Reliability aspects

Although buckling phenomenon, stiction due to friction and cracks during functioning have been avoided thanks to the use of simulation steps, the presented microgripper is the prey to some reliability problems, particularly in the actuation stage. The first one concerns the link motor/amplification mechanism; the difference of thickness (0.5 μm for the SDAs train, 4.5 μm for the amplification stage) increases the brittleness of the area and can cause the fracture of the polysilicon layer during the releasing step in the HF liquid. Moreover, not to use planarization steps during fabrication induces too the increase of brittleness in the moving pin-joints area due to step covering (Fig. 6b) [12]. Finally, SDA is an actuator based on friction, a phenomenon that can limit the lifetime of the motor. The last point is not inevitably a problem according to the final goal of the micro-actuator.

8. Conclusion

A novel technique for a microgripper has been demonstrated. The concept consists in combining a linear motor and an amplification stage in order to obtain a large stroke actuator. Electrostatic actuation of the gripper has been successfully obtained. The displacements in quasi-static mode have been performed thanks to the use of SDAs that allow a very precise positioning of the jaws. A permanent position kept by the jaws is obtained after the grasp of the object. Moreover, different simulations have determined the force generated in step with the grasped object stiffness, showing that shell elements for mesh were more suitable to get results. The influence of the geometric parameters (shape of the jaws and arms) on the kinematics parameters has been demonstrated. A complete system has been successfully realized and kinematics characterization has been done with different used topologies. This high precision, low-consumption, IC-compatible technique opens new capabilities, performances and application for biological analysis and safe transportation.

Acknowledgements

The authors would like to thank Pr. H. Fujita and his laboratory members from IIS, the University of Tokyo as well as Dr. T. Akiyama to transfer SDA technology to IEMN. The authors would like to thanks in the same way the valuable work of the IEMN technical staff and the ‘Délégation Générale de l’Armement’ for the financial support in 2002–2003.

References

[1] C.J. Kim, A.P. Pisano, R. Muller, Silicon-processed overhanging microgripper, J. Microelectromech. Syst. 1 (1992) 31.

[2] B.E. Volland, H. Heerlein, I.W. Rangelow, Electrostatically driven microgripper, Microelectron. Eng. 61–62 (2002) 1015–1023.

[3] S. Takeuchi, I. Shimoyama, A three-dimensional SMA microelectrodes with clipping structure for insect neural recording, J. Microelectromech. Syst. 9 (2000) 9–24.

[4] P. Krulevitch, A.P. Lee, P.B. Ramsey, J.C. Trevino, J. Hamilton, A. Northrup, Thin film shape memory alloy microactuators, J. Microelectromech. Syst. 5 (1996) 270.

[5] I. Roch, Ph. Bidaud, D. Collard, L. Buchaillot, Fabrication and characterization od an SU-8 gripper actuated by a shape memory alloy thin film, J. Micromech. Microeng. 13 (2003) 330–336.

[6] M.C. Carroza, A. Menciassi, G. Tiezzi, P. Dario, The development of a LIGA-microfabricated gripper for micromanipulation tasks, J. Micromech. Microeng. 8 (1998) 141.

[7] S. Bütefisch, V. Seidemann, S. Büttgenbach, Novel micro-pneumatic actuator for MEMS, Sens. Actuators A 97–98 (2002) 638–645.

[8] V. Seidemann, S. Bütefish, S. Büttgenbach, Fabrication and investigation of in-plane compliant SU8 structures for MEMS and their application to micro valves and micro grippers, Sens. Actuators A 97–98 (2002) 457–461.

[9] T. Akiyama, D. Collard, H. Fujita, Scratch drive actuator with mechanical links for self- assembly of three-dimensional MEMS, J. Microelectromech. Syst. 6 (1997) 10–17.

[10] C.H. Mastrangelo, C.H. Hsu, Mechanical stability and adhesion of microstructures under capillary forces—Part I: basic theory, J. Microelectromech. Syst. 2 (1993) 33–43.

[11] C.H. Mastrangelo, C.H. Hsu, Mechanical stability and adhesion of microstructures under capillary forces—Part II: experiments, J. Microelectromech. Syst. 2 (1993) 44–55.

[12] O. Millet, B. Legrand, D. Collard, L. Buchaillot, Influence of the step covering on fatigue phenomenon for polycrystalline silicon micro-electro-mechanical-systems (MEMS), Jpn. J. Appl. Phys. 41 (2002) 1339–1341.

Biographies

Olivier Millet received the Engineering degree from ISEN, and the Diplôme d’Etude Approfondies (DEA) in electrical engineering and computer science from the University of Science and Technology de Lille, France, both in 2000. He is currently working toward the PhD degree in electrical engineering at USTL. His research interests include failure modes of silicon MEMS microstructures, quality of materials, reliability of MEMS systems and microactuators.

Paul Bernardoni received the “Magistère” of technology and mechanics (similar to MS degree) from “Ecole Normale Supérieure” of Cachan, University of Paris VI, France in 2000 and is currently pursuing the PhD degree at the “Commissariat à l’Energie Atomique” and the “Laboratoire de Robotique de Paris”. His research interests are design of compliant mechanisms, medical robotics and micro robotics.

Stéphane Regnier received his PhD degree in Mechanics and Robotics from the University Pierre et Marie Curie, Paris, France in 1996. He is currently Associate Professor at the Laboratory of Robotics of Paris. His research interests are focused to microscale phenomenon, such as compliant mechanisms, micromechatronics and biological cell micromanipulation.

Philippe Bidaud is since 1999, professor at the Universite Pierre et Marie Curie, Paris 6. Since 1986, his field of research cover robotics and micro-robotics, from the point of view of mechanics. He is at the head of the Laboratoire de Robotique de Paris UPMC/CNRS.

Elli Tsitsiris received the “License” of technology and mechanics (similar to BSc degree) from “Ecole Normale Supérieure” of Cachan, University of Paris VI, France in 2002 and is currently pursuing the MS degree at the University of Paris VI.

Dominique Collard received the Engineering Degree from ISEN in 1980, and the PhD Degree from the University of Lille in 1984. from 1985 to 1986, he was with Toshiba ULSI research center in Kawasaki, Japan, as visiting scientist. He entered the Centre National de la Recherche Scientifique (CNRS) as senior researcher in 1988, and settled a research group on process and device simulation at ISEN, Lille, France. His own research activity focused on silicon oxidation simulation and related stress effects. In 1995–1997, he was director of the Laboratory For Integrated

MicroMechatronics Systems (LIMMS-CNRS-IIS), Tokyo, Japan, a joint CNRS laboratory with the Institute of Industrial Science of the University of Tokyo. Within LIMMS he worked on silicon based electrostatic actuator for device alignment system and self-assembling 3D technology. From 1997, he is with IEMN, as CNRS research director and settled a silicon micro-system group, working on micro-actuators and their integration in silicon micro-technology. From November 2000, he is also director of the CIRMM/CNRS (Center for International Research on MicroMechatronics) a joint center between IIS, The University of Tokyo and the CNRS to promote joint projects between French and Japan laboratories.

Lionel Buchaillot, received the Diplôme d'Etudes Approfondies (DEA) degree in materials science in 1991, and the PhD degree in mechanical engineering on the theoretical modeling of travelling wave piezoelectric motors in 1995 from the Université de Franche-Comté, Besançon. From 1995 to 1997, he has been with the Laboratory for Integrated MicroMechatronics Systems (LIMMS-CNRS-IIS) as a Japanese Society for the Promotion of Science (JSPS) Fellow working on thin film shape memory alloys (SMA) micro actuators for MEMS. In 1997, he worked for the R&D of the SFIM company (now SAGEM) and AVIAC technologies company. In 1998, he joined the CNRS in the ISEN department of the IEMN, Lille, France. Now, he is the head of the 'silicon-based MEMS' research group at IEMN. His research focused on thin film SMA for MEMS; MEMS for telecommunications (RF MEMS, MOEMS), and the MEMS reliability.